CHAPTER 10

Reactors Accomplishing Heterogeneous Reactions

10.1 | Homogeneous versus Heterogeneous Reactions in Tubular Reactors

In earlier chapters, tubular reactors of several forms have been described (e.g., laminar flow, plug flow, nonideal flow). One of the most widely used industrial reactors is a tubular reactor that is packed with a solid catalyst. This type of reactor is called a *fixed-bed* reactor since the solid catalyst comprises a bed that is in a fixed position. Later in this chapter, reactors that have moving, solid catalysts will be discussed.

A complete and perfect model for a fixed-bed reactor is not technically possible. However, such a model is not necessary. Rather, what is needed is a reasonably good description that accounts for the major effects. In this chapter, the fixed-bed reactor is analyzed at various degrees of sophistication and the applicability of each level of description is discussed.

Consider the PFR illustrated in Figure 10.1.1a. A mass balance on the reactor volume located within dz can be written as:

$$F_i = F_i + dF_i + (-\upsilon_i)\mathrm{r}dV \tag{10.1.1}$$

Since $F_i = uA_C C_i$ and $V = A_C z$, Equation (10.1.1) gives:

$$-u\frac{dC_i}{dz} = (-\upsilon_i)\mathrm{r} \tag{10.1.2}$$

provided u and A_C are not functions of z. The units of r are moles/(time · volume). Now let the tube be packed with a solid catalyst and write the material balance again (situation depicted in Figure 10.1.1b):

$$F_i = F_i + dF_i + \eta_o \rho_B (-\upsilon_i)\mathrm{r}dV \tag{10.1.3}$$

where the units on r (rate of reaction over the solid catalyst) are now mole/(mass of catalyst)/(time) and ρ_B is the bed density (mass of catalyst)/(volume of bed). Equation (10.1.3) can be written as:

$$-u\frac{dC_A}{dz} = \eta_o \rho_B (-\upsilon_i)\mathrm{r} \tag{10.1.4}$$

provided u and A_C are not functions of z. Note the differences between the PFR accomplishing a homogeneous [Equation (10.1.2)] and a solid catalyzed [Equation (10.1.4)] reaction. First of all, the solid-catalyzed reaction rate is per unit mass of catalyst and must therefore be multiplied by the bed density to obtain a reaction rate per unit volume in the mass balance. This is because the amount of catalyst packed into a reactor can vary from packing to packing with even the same solid. Thus, the bed density must be elucidated after each packing of the reactor, while the reaction rate per mass of catalyst need not be. Second, as discussed in Chapter 6, the overall effectiveness factor can be used to relate the reaction rate

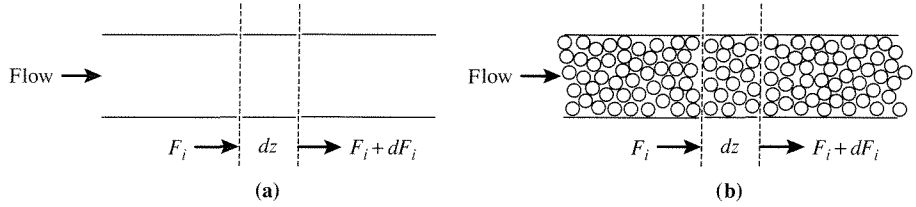

Figure 10.1.1 |
Illustrations of tubular reactors: **(a)** unpacked tube, **(b)** packed tube. $F_i = C_i\mathrm{v} = uA_CC_i$.

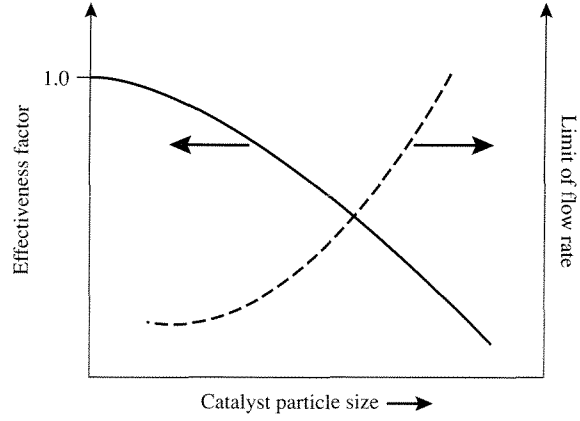

Figure 10.1.2 |
Effects of catalyst particle size on η_o and limits of flow rates.

that occurs within the catalyst particle to the rate that would occur at the local, bulk fluid conditions.

To maximize the reaction rate in the fixed-bed reactor, η_o should be equal to one. In order to do this, smaller particles are necessary (see Chapter 6). As the catalyst particles get smaller, the pressure drop along the reactor increases. (For example, ponder the differences in how difficult it is to have water flow through a column of marbles versus a column of sand.) Thus, a major consideration in the design of a fixed-bed reactor is the trade-off between pressure drop and transport limitations of the rate (illustrated in Figure 10.1.2). A practical design typically involves $\eta_o \neq 1$. Methodologies used to describe fixed-bed reactors given this situation are outlined in the next section.

10.2 | One-Dimensional Models for Fixed-Bed Reactors

Consider a PFR operating at nonisothermal conditions and accomplishing a solid-catalyzed reaction (Figure 10.1.1b). If the fluid properties do not vary over the cross-section of the tube, then only changes along the axial direction need to be considered. If such is the case, then the mass, energy, and momentum balances for a fixed-bed reactor accomplishing a single reaction can be written as:

$$\left.\begin{aligned} -u\frac{dC_i}{dz} &= \eta_o \rho_B (-v_i)\mathrm{r} && \text{(mass)} \\ u\rho\bar{C}_p\frac{dT}{dz} &= (-\Delta H_r|_{T^0})\eta_o\rho_B(-v_i)\mathrm{r} - \frac{4U}{d_t}(T - T^*) && \text{(energy)} \\ -\frac{dP}{dz} &= \frac{f_f \rho u^2}{g_c d_p} && \text{(momentum)} \\ C_i &= C_i^0, \quad T = T^0, \quad P = P^0 \text{ at } \quad z = 0 \end{aligned}\right\} \tag{10.2.1}$$

where u and A_C are not functions of z, f_f is a friction factor, and g_c is the gravitational constant. Mass and energy balances of this type were discussed in Chapter 9 for homogeneous reactions [Equation (9.4.9)] and their solutions were illustrated (Example 9.4.3). Here, the only differences are the use of the heterogeneous reaction rate terms and the addition of the momentum balance.

For packed columns with single-phase flow, the Ergun equation can be used for the momentum balance and is:

$$f_f = \frac{1 - \bar{\varepsilon}_B}{(\bar{\varepsilon}_B)^3}\left[1.75 + 150\frac{(1 - \bar{\varepsilon}_B)}{Re}\right] \tag{10.2.2}$$

where $\bar{\varepsilon}_B$ is the void fraction (porosity) of the bed and the Reynolds number is based on the particle size, d_p. The Ergun equation only considers frictional losses because of the packing. However, for $d_t/d_p < 50$, frictional losses from the wall of the tube are also significant. D. Mehta and M. C. Hawley [*Ind. Eng. Chem. Proc.*

Des. Dev., **8** (1969) 280] provided a correction factor to the Ergun equation to consider both the frictional losses from the wall and the packing, and their friction factor expression is:

$$f_f = \left[\frac{1-\bar{\varepsilon}_B}{(\bar{\varepsilon}_B)^3}\right]\left[1+\frac{2d_p}{3(1-\bar{\varepsilon}_B)d_t}\right]^2\left[\frac{1.75}{\left[1+\frac{2d_p}{3(1-\bar{\varepsilon}_B)d_t}\right]}+150\frac{(1-\bar{\varepsilon}_B)}{Re}\right] \quad (10.2.3)$$

Solution of Equation (10.2.1) provides the pressure, temperature, and concentration profiles along the axial dimension of the reactor. The solution of Equation (10.2.1) requires the use of numerical techniques. If the linear velocity is not a function of z [as illustrated in Equation (10.2.1)], then the momentum balance can be solved independently of the mass and energy balances. If such is not the case (e.g., large mole change with reaction), then all three balances must be solved simultaneously.

EXAMPLE 10.2.1

J. P. Kehoe and J. B. Butt [*AIChE J.*, **18** (1972) 347] have studied the kinetics of benzene hydrogenation on a Ni/kieselguhr catalyst. In the presence of excess dihydrogen, the reaction rate is given by:

$$r_B = P_{H_2} k_o K_o \exp\left[\frac{2700(\text{cal/mol})}{R_g T}\right] C_B \qquad (\text{mol/gcat/s})$$

where

$$k_o = 4.22 \text{ mol/(gcat-s-torr)}$$
$$K_o = 1.11 \times 10^{-3} \text{ cm}^3/\text{(mol)}$$
$$P_{H_2} = \text{in torr}$$

T. H. Price and J. B. Butt [*Chem. Eng. Sci.*, **32** (1977) 393] investigated this reaction in an adiabatic, fixed-bed reactor. Using the following data:

$$P_{H_2} = 685 \text{ torr}$$
$$\rho_B = 1.2 \text{ gcat/cm}^3$$
$$L/u = 0.045 \text{ s}$$
$$T^0 = 150°\text{C}$$
$$\overline{C}_p = 1.22 \times 10^5 \text{ J/(kmol-°C)}$$
$$-\Delta H_r|_{T^0} = 2.09 \times 10^8 \text{ J/kmol}$$

calculate the dimensionless concentration of benzene and the dimensionless temperature along the axial reactor dimension assuming $\eta_o = 1$.

■ Answer

The mass and energy balances can be written as (assume u is constant to simplify the solution of the material and energy balances):

$$-u\frac{dC_B}{dz} = \rho_B r_B$$

$$u\rho\bar{C}_p\frac{dT}{dz} = (-\Delta H_r|_{T^0})\rho_B r_B$$

$$C_B = C_B^0, \quad T = T^0 \text{ at } z = 0$$

Let $y = C_B/C_B^0$, $\bar{\theta} = T/T^0$ and $Z = z/L$, so that the mass and energy balances can be expressed as:

$$-\left(\frac{u}{L}\right)\frac{dy}{dZ} = \left(\rho_B \Big/ C_B^0\right) r_B$$

$$\rho\bar{C}_p\left(\frac{u}{L}\right)\frac{d\bar{\theta}}{dZ} = (-\Delta H_r|_{T^0})\left(\frac{\rho_B}{T^0}\right) r_B$$

$$y = \bar{\theta} = 1 \text{ at } Z = 0$$

Using the data given, the mass and energy balances reduce to (note that $C_B^0 \simeq 0.1\, C_{\text{total}} = 0.1\rho$):

$$\frac{dy}{dZ} = -0.174 \exp\left[\frac{3.21}{\bar{\theta}}\right] y$$

$$\frac{d\bar{\theta}}{dZ} = 0.070 \exp\left[\frac{3.21}{\bar{\theta}}\right] y$$

$$y = \bar{\theta} = 1 \text{ at } Z = 0$$

Numerical solution of these equations gives the following results:

Z	y	$\bar{\theta}$
0.0	1.00	1.00
0.1	0.70	1.12
0.2	0.53	1.19
0.3	0.41	1.23
0.4	0.33	1.27
0.5	0.27	1.29
0.6	0.22	1.31
0.7	0.18	1.33
0.8	0.15	1.34
0.9	0.12	1.35
1.0	0.10	1.36

Thus, at the reactor exit $C_B = 0.1C_B^0$ and $T = 302°C$.

Example 10.2.1 illustrates the simultaneous solution of the mass and energy balances for an adiabatic, fixed-bed reactor with no fluid density changes and no transport limitations of the rate, that is, $\eta_o = 1$. Next, situations where these simplifications do not arise are described.

If there is significant mole change with reaction and/or large changes in fluid density because of other factors such as large temperature changes, then Equation (10.2.1) is not appropriate for use. If the fluid density varies along the axial reactor dimension, then the mass and energy balances can be written as:

$$\left.\begin{aligned} -\frac{dF_A}{dz} &= A_C\,\eta_o\rho_B(-\upsilon_A)\mathrm{r} \\ \frac{d}{dz}\left(\sum_i F_i C_{p_i} T\right) &= A_C(-\Delta H_r|_{T^0})\eta_o\rho_B(-\upsilon_A)\mathrm{r} - \frac{4UA_C}{d_t}(T - T^*) \end{aligned}\right\} \tag{10.2.4}$$

Recall that:

$$\begin{aligned} \mathrm{v} &= A_C u \\ F_A &= F_A^0(1 - f_A) \\ F_A &= \mathrm{v}C_A = \mathrm{v}_0(1 + \varepsilon_A f_A)\left[C_A^0\left(\frac{1 - f_A}{1 + \varepsilon_A f_A}\right)\right]\left(\frac{P^0}{P}\right)\left(\frac{T}{T^0}\right) \\ \sum_i F_i C_{p_i} &= \mathrm{v}\rho\overline{C}_p \end{aligned}$$

Using these expressions in Equation (10.2.4) gives:

$$\left.\begin{aligned} -\frac{dF_A}{dz} &= A_C\,\eta_o\rho_B(-\upsilon_A)\mathrm{r} \\ u\rho\overline{C}_p\frac{dT}{dz} &= (-\Delta H_r|_{T^0})\eta_o\rho_B(-\upsilon_A)\mathrm{r} - \frac{4U}{d_t}(T - T^*) \\ -\frac{dP}{dz} &= \frac{f_f\rho u^2}{g_c d_p} \\ F_A &= F_A^0, \quad T = T^0, \quad P = P^0 \quad \text{at} \quad z = 0 \end{aligned}\right\} \tag{10.2.5}$$

assuming $\overline{C}_p$ is not a strong function of T. All three balances in Equation (10.2.5) must be solved simultaneously, since $u = u_o(1 + \varepsilon_A f_A)(P^0/P)(T/T^0)$.

Thus far, the overall effectiveness factor has been used in the mass and energy balances. Since η_o is a function of the local conditions, it must be computed along the length of the reactor. If there is an analytical expression for η_o, for example for an isothermal, first-order reaction rate:

$$\eta_o = \frac{\tanh(\phi)}{\phi\left[1 + \dfrac{\phi\tanh(\phi)}{Bi_m}\right]} \tag{6.4.34}$$

then the use of η_o is straightforward. As the mass and energy balances are being solved along the axial reactor dimension, η_o can be computed by calculating ϕ and Bi_m at each point. The assumption of an isothermal η_o may be appropriate since it is calculated at each point along the reactor. That is to say that although the temperature varies along the axial direction, at each point along this dimension, the catalyst particle may be isothermal (e.g., at $Z = 0$, $\eta_o = \eta_o(T^0)$ and at $Z \neq 0$, $\eta_o = \eta_o(T) \neq \eta_o(T^0)$).

For most solid-catalyzed reactions, there will not be analytical solutions for η_o. In this case, the effectiveness factor problem must be computed at each point in the reactor. The reactor balances like those given in Equation (10.2.1) that now incorporate the effectiveness factor description are:

Bulk Fluid Phase:

$$\left.\begin{aligned} -u\frac{dC_{AB}}{dz} &= \bar{k}_c\, a_v\,(C_{AB} - C_{AS}) \\ u\rho\,\bar{C}_p\frac{dT_B}{dz} &= h_t a_v(T_S - T_B) - \frac{4U}{d_t}(T_B - T^*) \\ -\frac{dP}{dz} &= \frac{f_f \rho u^2}{g_c d_p} \\ C_{AB} = (C_{AB})^0, \quad T_B = (T_B)^0, \quad P &= P^0 \quad \text{at} \quad Z = 0 \end{aligned}\right\} \tag{10.2.6}$$

Solid Phase (Spherical Catalyst Particle):

$$\left.\begin{aligned} D^e\left(\frac{d^2C_A}{d\bar{r}^2} + \frac{2}{\bar{r}}\frac{dC_A}{d\bar{r}}\right) &= \rho_p\,(-\upsilon_A)\mathrm{r}\,(C_A, T) \\ \lambda^e\left(\frac{d^2T}{d\bar{r}^2} + \frac{2}{\bar{r}}\frac{dT}{d\bar{r}}\right) &= (-\Delta H_r)\,\rho_p\,(-\upsilon_A)\mathrm{r}\,(C_A, T) \end{aligned}\right\} \tag{10.2.7}$$

with

$$\frac{dT}{d\bar{r}} = \frac{dC_A}{d\bar{r}} = 0 \quad \text{at} \quad \bar{r} = 0$$

$$\bar{k}_c(C_{AS} - C_{AB}) = -D^e\frac{dC_A}{d\bar{r}} \quad \text{at} \quad \bar{r} = R_p$$

$$h_t(T_S - T_B) = -\lambda^e\frac{dT}{d\bar{r}} \quad \text{at} \quad \bar{r} = R_p$$

where

$$T = T_S \quad \text{at} \quad \bar{r} = R_p$$
$$C_A = C_{AS} \quad \text{at} \quad \bar{r} = R_p$$

and

C_{AB}, T_B = bulk fluid phase concentration of A and temperature

ρ_p = density of the catalyst particle

a_v = external catalyst particle surface area per unit reactor volume

Notice how the catalyst particle balances are coupled to the reactor mass and energy balances. Thus, the catalyst particle balances [Equation (10.2.7)] must be solved at each position along the axial reactor dimension when computing the bulk mass and energy balances [Equation (10.2.6)]. Obviously, these solutions are lengthy.

Since most practical problems do not have analytical expressions for the effectiveness factor, the use of Equations (10.2.6) and (10.2.7) are more generally applicable. If Equations (10.2.6) and (10.2.7) are to be solved numerous times (e.g., when performing a reactor design/optimization), then an alternative approach may be applicable. The catalyst particle problem can first be solved for a variety of C_{AB}, T_B, ϕ, Bi_m, Bi_h that may be expected to be realized in the reactor design. Second, the η_o values can be fit to a function with C_{AB}, T_B, ϕ, Bi_m, Bi_h as variables, that is,

$$\eta_o = \eta_o(C_{AB}, T_B, \phi, Bi_m, Bi_h) \tag{10.2.8}$$

Finally, using the function (normally nonlinear) for η_o in Equation (10.2.1) allows a more efficient numerical solution of the reactor balances.

VIGNETTE 10.2.1

In Example 3.4.3, it was shown that the solution to the PFR mass balance can be obtained by using a series of CSTRs provided the number within the series is sufficiently large. This approach can be used to solve reactor descriptions like Equation (10.2.1) and Equations (10.2.6) and (10.2.7). Since numerical software for solving Equation (10.2.1) and Equations (10.2.6) and (10.2.7) is now readily available it is less likely that the conversion of these differential equations into systems of algebraic equations (series of CSTRs) is necessary. However, there may be situations where this approach is preferred. When doing so it is advisable to always check for the number of stages (CSTRs) that are necessary for solution. As an example of this approach, refer to the reactor situation provided in Vignette 8.5.1. Simulation of the plug flow model of the fixed-film bioreactor was performed by transforming the reactor description into a series of CSTR equations. The solution of these equations is illustrated in Figure 10.2.1 [from Y. Park et al., *Biotech. Bioeng.*, **26** (1984) 457].

Note the differences in the solution for the number of stages (NSTAGE) (i.e., CSTRs) less than 50. Although not shown, all solutions using 50 or greater CSTRs were indistinguishable. Once the number of stages necessary for solution is identified, then the reactor simulations can be performed.

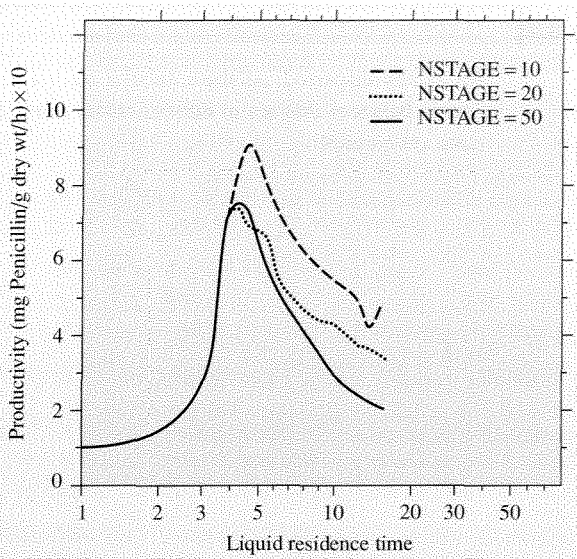

Figure 10.2.1 | Plug flow reactor simulation using NSTAGEs of CSTRs for solution. [From "Analysis of a Continuous, Aerobic Fixed-Film Bioreactor. I. Steady-State Behavior," by Y. Park, M. E. Davis and D. A. Wallis, *Biotech. Bioeng.*, **26** (1984) 457, copyright © 1984, Wiley-Liss, Inc., a subsidiary of John Wiley and Sons, Inc.]

In Chapter 8, axial dispersion in tubular reactors was discussed. Typical industrial reactors have sufficiently high flow rates and reactor lengths so the effects of axial dispersion are minimal and can be neglected. A rule of thumb is that axial dispersion can be neglected if:

$$L/d_p > 50 \qquad \text{isothermal}$$
$$L/d_p > 150 \qquad \text{nonisothermal}$$

Additionally, L. C. Young and B. A. Finlayson [*Ind. Eng. Chem. Fund.*, **12** (1973) 412] showed that if:

$$\left| \frac{\eta_o(-\upsilon_A)\mathrm{r}\rho_B d_p}{uC_{AB}} \right| \ll \left| \frac{ud_p}{D_a} \right| = Pe_a$$

then axial dispersion can be neglected. However, for laboratory reactors that can have low flow rates and are typically of short axial length, axial dispersion may become important. If such is the case, then the effects of axial dispersion may be needed to accurately describe the reactor.

EXAMPLE 10.2.2

An axially-dispersed, adiabatic tubular reactor can be described by the following mass and energy balances that are in dimensionless form (the reader should verify that these descriptions are correct):

$$\frac{1}{Pe_a}\frac{d^2y}{dZ^2} - \frac{dy}{dZ} - \mathrm{r}(y,\bar{\theta}) = 0$$

$$\frac{1}{Bo_a}\frac{d^2\bar{\theta}}{dZ^2} - \frac{d\bar{\theta}}{dZ} - \bar{H}_w\mathrm{r}(y,\bar{\theta}) = 0$$

with

$$\frac{1}{Pe_a}\frac{dy}{dZ} = y - 1 \quad \text{at} \quad Z = 0$$

$$\frac{1}{Bo_a}\frac{d\bar{\theta}}{dZ} = \bar{\theta} - 1 \quad \text{at} \quad Z = 0$$

$$\frac{dy}{dZ} = 0 \quad \text{at} \quad Z = 1$$

$$\frac{d\bar{\theta}}{dZ} = 0 \quad \text{at} \quad Z = 1$$

If $\bar{H}_w = -0.05$, and $\mathrm{r}(y,\bar{\theta}) = 4y\exp\left[18\left(1 - \frac{1}{\bar{\theta}}\right)\right]$, calculate y and $\bar{\theta}$ for $Pe_a = Bo_a = 10$, 20, and 50 (Bo_a is a dimensionless group analogous to the axial Peclet number for the energy balance).

■ Answer

The dimensionless system of equations shown above are numerically solved to give the following results.

	$Pe_a = 10$		$Pe_a = 20$		$Pe_a = 50$	
Z	y	$\bar{\theta}$	y	$\bar{\theta}$	y	$\bar{\theta}$
0.0	0.707	1.01	0.824	1.01	0.923	1.00
0.2	0.276	1.03	0.293	1.04	0.309	1.03
0.4	0.092	1.05	0.082	1.05	0.072	1.05
0.6	0.029	1.05	0.021	1.05	0.015	1.05
0.8	0.009	1.05	0.005	1.05	0.003	1.05
1.0	0.004	1.05	0.002	1.05	0.001	1.05

As $Pe_a \to \infty$ the reactor behavior approaches PFR. From the results illustrated, this trend is shown (for PFR, $y = \bar{\theta} = 1$ at $Z = 0$).

In general, a one-dimensional description for fixed-bed reactors can be used to capture the reactor behavior. For nonisothermal reactors, the observation of hot spots (see Example 9.4.3) and reactor stability (see Example 9.6.2) can often be described.

However, there are some situations where the one-dimensional descriptions do not work well. For example, with highly exothermic reactions, a fixed-bed reactor may contain several thousand tubes packed with catalyst particles such that $d_t/d_p \sim 5$ in order to provide a high surface area per reaction volume for heat transfer. Since the heat capacities of gases are small, radial temperature gradients can still exist for highly exothermic gas-phase reactions, and these radial variations in temperature produce large changes in reaction rate across the radius of the tube. In this case, a two-dimensional reactor model is required.

10.3 | Two-Dimensional Models for Fixed-Bed Reactors

Consider a tubular fixed-bed reactor accomplishing a highly exothermic gas-phase reaction. Assuming that axial dispersion can be neglected, the mass and energy balances can be written as follows and allow for radial gradients:

$$\left.\begin{aligned} \frac{\partial}{\partial z}(uC_A) - \frac{1}{\bar{r}}\frac{\partial}{\partial \bar{r}}\left(\bar{r}D_r\frac{\partial C_A}{\partial \bar{r}}\right) + \eta_o\rho_B(-v_A)\mathrm{r} = 0 \\ \frac{\partial}{\partial z}(u\rho\bar{C}_pT) - \frac{1}{\bar{r}}\frac{\partial}{\partial \bar{r}}\left(\bar{r}\bar{\lambda}_r\frac{\partial T}{\partial \bar{r}}\right) + (-\Delta H_r)\eta_o\rho_B(-v_A)\mathrm{r} = 0 \end{aligned}\right\} \quad (10.3.1)$$

where D_r is the radial dispersion coefficient (see Chapter 8) and $\bar{\lambda}_r$ is the effective thermal conductivity in the radial direction. If D_r and $\bar{\lambda}_r$ are not functions of $\bar{r}$ then Equations (10.3.1) can be written as (u not a function of z):

$$\left.\begin{aligned} u\frac{\partial C_A}{\partial z} &= D_r\left[\frac{\partial^2 C_A}{\partial \bar{r}^2} + \frac{1}{\bar{r}}\frac{\partial C_A}{\partial \bar{r}}\right] - \eta_o\rho_B(-v_A)\mathrm{r} \\ u\rho\bar{C}_p\frac{\partial T}{\partial z} &= \bar{\lambda}_r\left[\frac{\partial^2 T}{\partial \bar{r}^2} + \frac{1}{\bar{r}}\frac{\partial T}{\partial \bar{r}}\right] - (-\Delta H_r)\eta_o\rho_B(-v_A)\mathrm{r} \end{aligned}\right\} \quad (10.3.2)$$

The conditions necessary to provide a solution to Equation (10.3.2) are:

$$\left.\begin{aligned} C_A &= C_A^0, \quad T = T^0 \quad \text{at} \quad z = 0 \quad \text{for} \quad 0 \le \bar{r} \le d_t/2 \\ \frac{\partial C_A}{\partial \bar{r}} &= \frac{\partial T}{\partial \bar{r}} = 0 \quad \text{at} \quad \bar{r} = 0 \quad \text{for} \quad 0 \le z \\ \frac{\partial C_A}{\partial \bar{r}} &= 0 \quad \text{at} \quad \bar{r} = d_t/2 \quad \text{for} \quad 0 \le z \\ -\bar{\lambda}_r\frac{\partial T}{\partial \bar{r}} &= h_t(T - T_w) \quad \text{at} \quad \bar{r} = d_t/2 \quad \text{for} \quad 0 \le z \end{aligned}\right\} \quad (10.3.3)$$

where h_t is the heat transfer coefficient at the reactor wall and T_w is the wall temperature. Solution of Equations (10.3.2) and (10.3.3) gives $C_A(\bar{r}, z)$ and $T(\bar{r}, z)$.

EXAMPLE 10.3.1

G. F. Froment [*Ind. Eng. Chem.*, **59** (1967) 18] developed a two-dimensional model for a fixed-bed reactor accomplishing the following highly exothermic gas phase reactions:

$$\underset{(A)}{\text{o-xylene}} \xrightarrow{k_1} \underset{(B)}{\text{phthalic anhydride}} \xrightarrow{k_2} \underset{(C)}{CO_2, CO, H_2O}$$

$$\text{o-xylene} \downarrow k_3 \quad \underset{(C)}{CO_2, CO, H_2O}$$

The steady-state mass and energy balances are (in dimensionless form):

$$\frac{\partial y_1}{\partial Z} = Pe_r\left[\frac{\partial^2 y_1}{\partial \bar{R}^2} + \frac{1}{\bar{R}}\frac{\partial y_1}{\partial \bar{R}}\right] + \beta\beta_1 r_1$$

$$\frac{\partial y_2}{\partial Z} = Pe_r\left[\frac{\partial^2 y_2}{\partial \bar{R}^2} + \frac{1}{\bar{R}}\frac{\partial y_2}{\partial \bar{R}}\right] + \beta\beta_1 r_2$$

$$\frac{\partial \bar{\theta}}{\partial Z} = Bo_r\left[\frac{\partial^2 \bar{\theta}}{\partial \bar{R}^2} + \frac{1}{\bar{R}}\frac{\partial \bar{\theta}}{\partial \bar{R}}\right] + \beta\beta_2 r_1 + \beta\beta_3 r_2$$

with

$$y_1 = y_2 = 0 \qquad \text{at} \quad Z = 0 \quad \text{for} \quad 0 \le \bar{R} \le 1$$

$$\bar{\theta} = 1 \qquad \text{at} \quad Z = 0 \quad \text{for} \quad 0 \le \bar{R} \le 1$$

$$\frac{\partial y_1}{\partial \bar{R}} = \frac{\partial y_2}{\partial \bar{R}} = \frac{\partial \bar{\theta}}{\partial \bar{R}} = 0 \qquad \text{at} \quad \bar{R} = 0 \quad \text{for} \quad 0 \le Z \le 1$$

$$\frac{\partial y_1}{\partial \bar{R}} = \frac{\partial y_2}{\partial \bar{R}} = 0 \qquad \text{at} \quad \bar{R} = 1 \quad \text{for} \quad 0 \le Z \le 1$$

$$\frac{\partial \bar{\theta}}{\partial \bar{R}} = \bar{H}_w\left(\bar{\theta}_w - \bar{\theta}\right) \qquad \text{at} \quad \bar{R} = 1 \quad \text{for} \quad 0 \le Z \le 1$$

where

$y_1 = C_B/C_A^0$
$y_2 = C_C/C_A^0$
$\bar{\theta}$ = dimensionless temperature
Z = dimensionless axial coordinate
$\bar{R}$ = dimensionless radial coordinate
$r_1 = k_1(1 - y_1 - y_2) - k_2 y_1$
$r_2 = k_2 y_1 + k_3(1 - y_1 - y_2)$
$\beta\beta_i$ = dimensionless groups
$\bar{\theta}_w$ = dimensionless wall temperature

Using the data given by Froment,

$$Pe_r = 5.706, Bo_r = 10.97, \overline{H}_w = 2.5$$

$$\beta\beta_1 = 5.106, \beta\beta_2 = 3.144, \beta\beta_3 = 11.16$$

Additionally,

$$k_1 = \exp\left[-1.74 + 21.6\left(1 - \frac{1}{\overline{\theta}}\right)\right]$$

$$k_2 = \exp\left[-4.24 + 25.1\left(1 - \frac{1}{\overline{\theta}}\right)\right]$$

$$k_3 = \exp\left[-3.89 + 22.9\left(1 - \frac{1}{\overline{\theta}}\right)\right]$$

If $\overline{\theta}_w = 1$, compute $y_1(Z, \overline{R})$, $y_2(Z, \overline{R})$ and $\overline{\theta}(Z, \overline{R})$.

■ Answer

This reactor description is a coupled set of parabolic partial differential equations that are solved numerically. The results shown here were obtained using the software package PDECOL [N. K. Madsen and R. F. Sincovec, *ACM Toms*, **5** (1979) 326].

Below are listed the radial profiles for two axial positions within the reactor. Notice that at $Z = 0.2$, there are significant radial gradients while by $Z = 0.6$ these gradients are all but eliminated. If the inlet and coolant temperatures are around 360°C, then the centerline and inner wall temperatures at $Z = 0.2$ are 417°C and 385°C, respectively, giving a radial temperature difference of 32°C.

	$Z = 0.2$		
$\overline{R}$	y_1	y_2	$\overline{\theta}$
0.0	0.458	0.782	1.09
0.2	0.456	0.777	1.09
0.4	0.451	0.763	1.08
0.6	0.445	0.747	1.07
0.8	0.440	0.734	1.05
1.0	0.438	0.728	1.04

	$Z = 0.6$		
$\overline{R}$	y_1	y_2	$\overline{\theta}$
0.0	0.613	0.124	1.02
0.2	0.613	0.124	1.02
0.4	0.613	0.124	1.01
0.6	0.612	0.124	1.01
0.8	0.612	0.124	1.01
1.0	0.612	0.124	1.01

As illustrated in Example 10.3.1, the radial temperature gradient can be significant for highly exothermic, gas-phase reactions. Therefore, one must make a decision for a particular situation under consideration as to whether a 1-D or 2-D analysis is needed.

10.4 | Reactor Configurations

Thus far, fixed-bed reactor descriptions have been presented. Schematic representations of fixed-bed reactors are provided in Figure 10.4.1, and a photograph of a commercial reactor is provided in Figure 10.4.2.

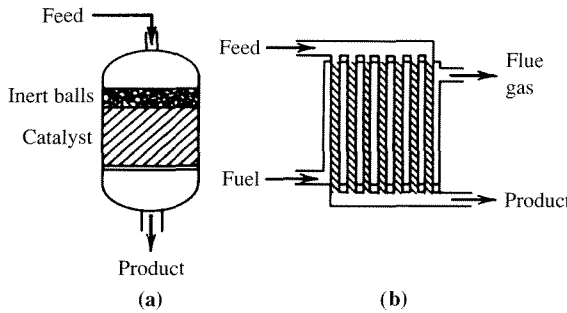

Figure 10.4.1 |
Fixed-bed reactor schematics: **(a)** adiabatic, **(b)** nonadiabatic. [From "Reactor Technology" by B. L. Tarmy, *Kirk-Othmer Encyclopedia of Chemical Technology,* vol. 19, 3rd ed., Wiley (1982). Reprinted by permission of John Wiley and Sons, Inc., copyright © 1982.]

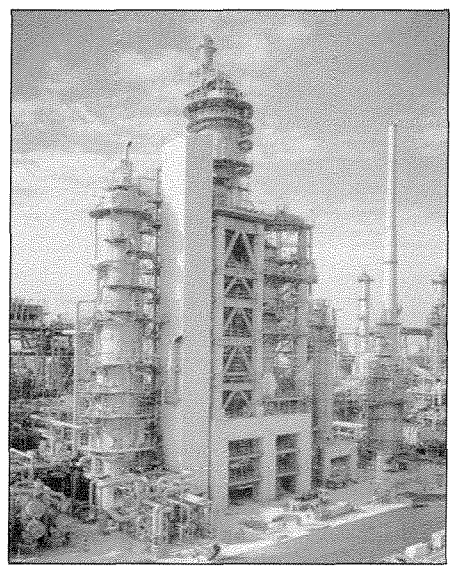

Figure 10.4.2 |
Photograph of a commercial reactor. (Image provided by T. F. Degnan of Exxon Mobil.)

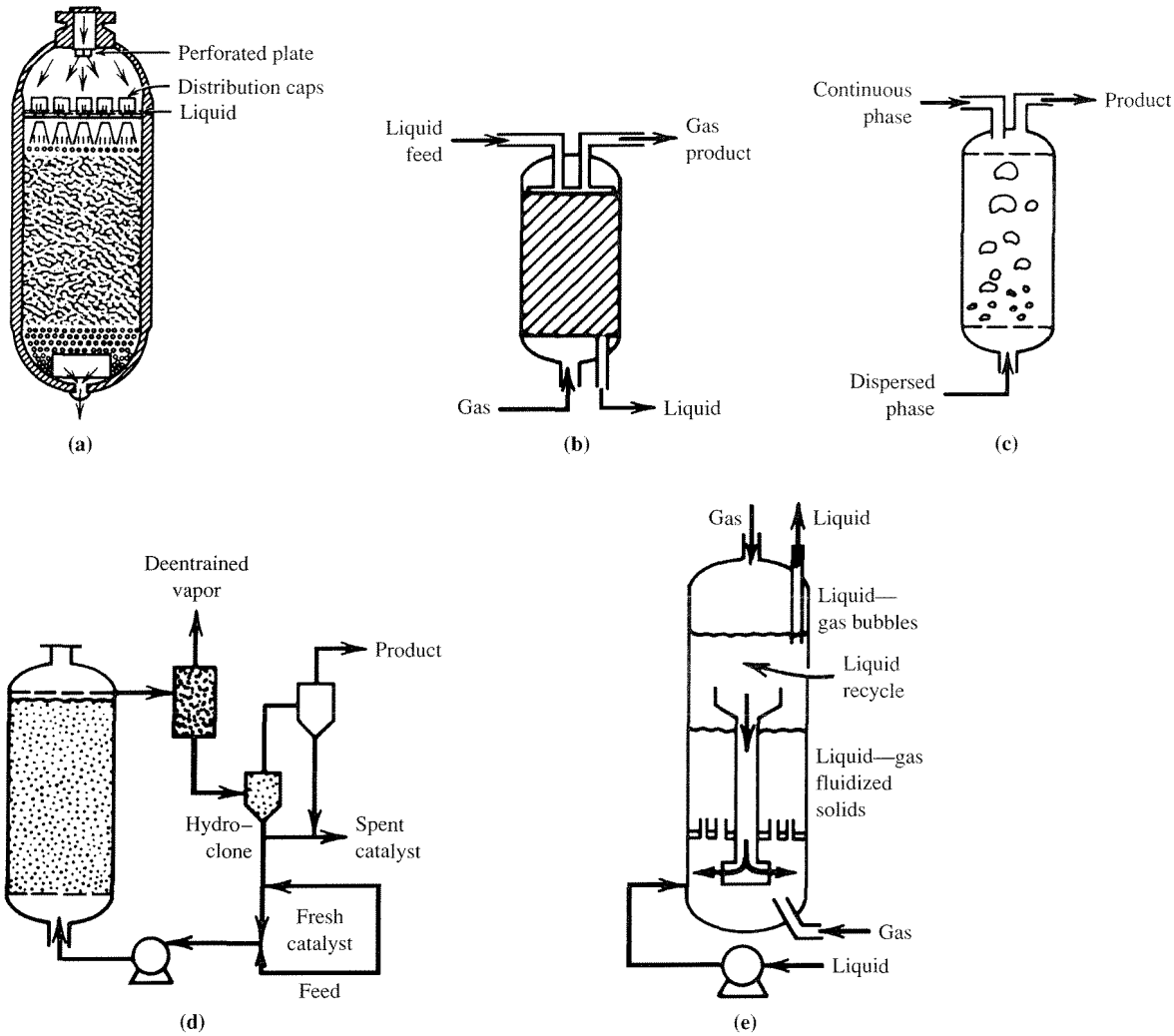

Figure 10.4.3 |
Examples of multiphase reactors: **(a)** trickle-bed reactor, **(b)** countercurrent packed-bed reactor, **(c)** bubble column, **(d)** slurry reactor, and **(e)** a gas-liquid fluidized bed. [From "Reactor Technology" by B. L. Tarmy, *Kirk-Othmer Encyclopedia of Chemical Technology*, vol. 19, 3rd ed., Wiley (1982). Reprinted by permission of John Wiley and Sons, Inc., copyright © 1982.]

The reactor models developed for fixed-bed reactors have been exploited for use in other situations, for example, CVD reactors (see Vignette 6.4.2) for microelectronics fabrication. These models are applicable to reaction systems involving single fluid phases and nonmoving solids. There are numerous reaction systems that involve more than one fluid phase. Figure 10.4.3 illustrates various types of reactors

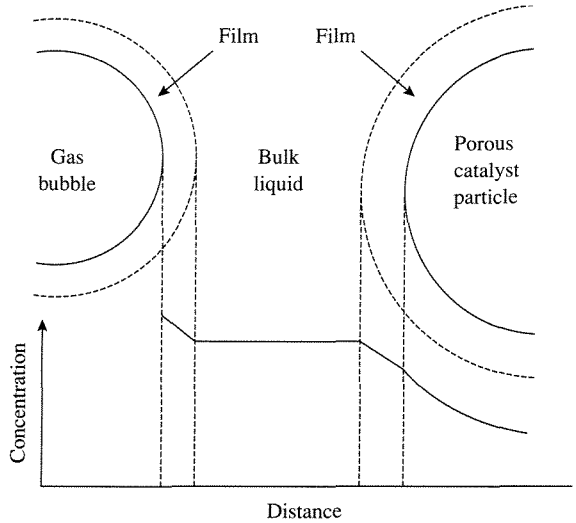

Figure 10.4.4 |
Concentration profile of a gas-phase reactant in a porous solid-catalyzed reaction occurring in a three phase reactor.

that process multiple fluid phases. Figure 10.4.3a shows a schematic of a trickle-bed reactor. In this configuration, the solid catalyst remains fixed and liquid is sprayed down over the catalyst to create contact. Additionally, gas-phase components can enter either the top (cocurrent) or the bottom (countercurrent; Figure 10.4.3b) of the reactors to create three-phase systems. The three-phase trickle-bed reactor provides large contact between the catalyst and fluid phases. Typical reactions that exploit this type of contact are hydrogenations (H_2—gas, reactant to be hydrogenated—liquid) and halogenations. Bubble (Figure 10.4.3c), slurry (Figure 10.4.3d), and fluidized (Figure 10.4.3e) reactors can also accomplish multiphase reactions (solid catalyst in liquid phase for both cases). As with all multiphase reactors, mass transfer between phases (see Figure 10.4.4) can be very important to their overall performance.

The mathematical analyses of these reactor types will not be presented here. Readers interested in these reactors should consult references specific to these reactor types.

VIGNETTE 10.4.1

Fixed-bed reactors are commonly employed by the petrochemicals industries to accomplish a broad spectrum of reactions, including steps to clean up air streams prior to exhausting them into the atmosphere. For example, fixed-bed reactors are used to process air streams containing NO_x by reaction with NH_3 over solid catalysts to give N_2 and H_2O. An interesting application of fixed-bed reactors for environmental cleanup is from workers

at Engelhard Corporation, who have developed fixed-bed reactors for treating cooking fumes (U.S. Patent 5,580,535). Exhaust plumes from fast food restaurants contain components that contribute to air pollution. Engelhard has implemented in some fast food restaurants a fixed-bed catalytic reactor to oxidize the exhaust components to CO_2. A second example where fixed beds are used to clean up exhaust streams involves wood stoves. In certain areas of the United States, the chimneys of wood stoves now contain fixed beds of catalysts to assist in the cleanup of wood stove fumes prior to their release into the atmosphere. These two examples show how the fixed-bed reactor is not limited to use in the petrochemical industries.

10.5 | Fluidized Beds with Recirculating Solids

Fluidized beds with recirculating solids developed primarily as reactors for the catalytic cracking of oil to gasoline. Today their uses are much broader. Prior to the early 1940s, catalytic cracking of oil was performed in fixed-bed reactors. After that time, fluidized-bed reactors have been developed for this application. Today, fluidized beds with recirculating zeolite-based catalysts are used for catalytic cracking of oil.

VIGNETTE 10.5.1

In the late 1950s and early 1960s, certain zeolites (Vignette 5.3.1) were found to be excellent catalysts for catalytic cracking. They were observed to improve yields to gasoline, and in the early 1960s the Mobil Corporation introduced the first zeolite-based, fluidized-bed catalytic cracking process. Virtually all refineries in the world use some variation of this theme for catalytic cracking. It has been claimed that the improved efficiency of cracking with zeolite catalysts has provided the United States with a savings of greater than 400 million barrels of oil per year. At $30 a barrel, this savings amounts to more than $12 billion a year.

Figure 10.5.1 shows a schematic of a fluidized bed with recirculating solids. The oil feed enters at the bottom of the riser reactor and is combined with the solid catalyst. The vapor moves upward through the riser at a flow rate sufficient to fluidize the solid catalyst and transport it to the top of the riser in a millisecond timeframe. The catalytic cracking reactions occur during the transportation of the solids to the top of the riser and the catalyst becomes covered with carbonaceous residue (coke) that deactivates it by that point. The solids are separated from the products and enter a fluidized-bed, regeneration reactor. In the regeneration reactor, the carbonaceous residue is removed from the catalyst by combustion with the oxygen in the air. The "clean" catalyst is then returned to the bottom of the riser reactor. Thus, the solid catalyst recirculates between the two reactors. Typical fluidized beds with recirculating solids contain around 250 tons of catalyst of 20–80 microns in particle

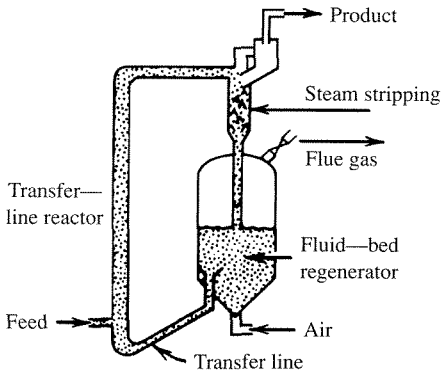

Figure 10.5.1 |
Schematic of fluidized-bed reactor with recirculating solids. [From "Reactor Technology" by B. L. Tarmy, *Kirk-Othmer Encyclopedia of Chemical Technology,* vol. 19, 3rd ed., Wiley (1982). Reprinted by permission of John Wiley and Sons, Inc., copyright © 1982.]

size and have circulation rates of around 25 ton/min. As might be expected, the solids are continuously being degraded into smaller particles that exit the reactor. Typical catalyst losses are around 2 ton/day for a catalyst reactor inventory of 250 ton. Thus, catalyst must be continually added.

The fluidized-bed reactor with recirculating solids is an effective reactor configuration for accomplishing reactions that have fast deactivation and regeneration. In addition to catalytic cracking, this configuration is now being used for another type of reaction. The oxidation of hydrocarbons can be accomplished with oxide-based catalysts. In the mid-1930s, Mars and van Krevelen postulated that the oxidation of hydrocarbons by oxide-containing catalysts could occur in two steps:

$$\textit{Overall:}\quad \underset{\text{(hydrocarbon)}}{RH_2} + O_2 \Rightarrow \underset{\text{(oxidized product)}}{RO} + H_2O$$

$$\textit{Step 1:}\quad RH_2 + \underset{\text{(lattice oxygen)}}{2O^{-2}} \Rightarrow RO + H_2O + 4e^- + \underset{\text{(surface oxygen vacancy)}}{2\square}$$

$$\textit{Step 2:}\quad O_2 + 2\square + 4e^- \Rightarrow 2O^{-2}$$

In the first step the hydrocarbon is oxidized by lattice oxygen from the oxide-containing catalyst to create surface oxygen vacancies in the oxide. The second step involves filling the vacancies by oxidization of the reduced oxide surface with

dioxygen. This mechanism has been shown to hold for numerous oxide-based catalytic oxidations.

Dupont has recently commercialized the reaction of n-butane to maleic anhydride using a vanadium phosphorus oxide (VPO) catalyst in a recirculating solid reactor system. The overall reaction is:

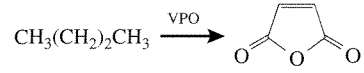

A proposed reaction pathway over the VPO catalyst is as shown below:

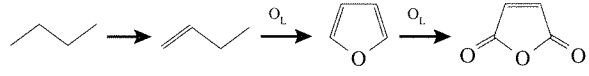

where O_L denotes lattice oxygen. In addition to these reactions, each of the organic compounds can be oxidized to CO_2 and CO. In the absence of gas-phase O_2 the selectivity to CO_2 and CO is minimized. A solids recirculating reactor system like that schematically illustrated in Figure 10.5.1 was developed to accomplish the butane oxidation. In the riser section, oxidized VPO is contacted with butane to produce maleic anhydride. The reduced VPO solid is then re-oxidized in the regeneration reactor. Thus, the VPO is continually being oxidized and reduced (Mars–van Krevelen mechanism). This novel reactor system opens the way to explore the performance of other gas-phase oxidations in solids recirculating reactors.

There are numerous other types of reactors (e.g., membrane reactors) that will not be discussed in this text. Readers interested in reactor configuration should look for references specific to the reactor configuration of interest.

Exercises for Chapter 10

1. Consider the reactor system given in Example 10.2.1.
   (a) Compare the dimensionless concentration profile from the adiabatic case given in the example to that obtained at isothermal conditions.
   (b) What happens if the reactor is operated adiabatically and the heat of reaction is doubled?
   (c) If the reactor in part (b) is now cooled with a constant wall temperature of 150°C, what is the value of $4U/d_t$ that is necessary to bring the outlet temperature to approximately the value given in Example 10.2.1?
2. Plot the dimensionless concentration and temperature profiles for the reactor system given in Example 10.2.2 for $Pe_a = Bo_a = \infty$ and compare them to those obtained when $Pe_a = Bo_a = 15$.
3. Reproduce the results given in Example 10.3.1. What happens as $\overline{H}_w$ is decreased?
4. Design a multitube fixed-bed reactor system to accomplish the reaction of naphthalene (N) with air to produce phthalic anhydride over a catalyst of vanadium pentoxide on silica gel at a temperature of about 610–673 K.

The selective oxidation reaction is carried out in excess air so that it can be considered pseudo-first-order with respect to naphthalene. Analysis of available data indicates that the reaction rate per unit mass of catalyst is represented by:

$$r = k_1 C_N \quad \text{with } k_1 = 1.14 \times 10^{13} \exp(-19{,}000/T) \ (\text{cm}^3\ \text{s}^{-1}\ \text{gcat}^{-1})$$

where C_N = the concentration of naphthalene in mol cm^{-3}, and T = absolute temperature in K. (Data for this problem were adapted from C. G. Hill, Jr. *An Introduction to Chemical Engineering Kinetics and Reactor Design,* Wiley, New York, 1977, p. 554.) Assume for this problem that the overall effectiveness factor is unity (although in reality this assumption is likely to be incorrect!). To keep the reactant mixture below the explosion limit of about 1 percent naphthalene in air, consider a feed composition of 0.8 mol % naphthalene vapor in 99.2 percent air at 1.7 atm total pressure. Although there will be some complete oxidation of the naphthalene to CO_2 and H_2O (see part c), initially assume that the only reaction of significance is the selective oxidation to phthalic anhydride as long as the temperature does not exceed 673 K anywhere in the reactor:

$$C_{10}H_8 + 4.5\ O_2 \Rightarrow C_8H_4O_3 + 2\ H_2O + 2\ CO_2$$

The heat of reaction is -429 kcal mol^{-1} of naphthalene reacted. The properties of the reaction mixture may be assumed to be equivalent to those of air (C_p = 0.255 cal $\text{g}^{-1}\ \text{K}^{-1}$, $\overline{\mu} = 3.2 \times 10^{-4}$ g $\text{cm}^{-1}\ \text{s}^{-1}$) in the temperature range of interest.

It is desired to determine how large the reactor tubes can be and still not exceed the maximum temperature of 673 K. The reactor will be designed to operate at 95 percent conversion of $C_{10}H_8$ and is expected to have a production rate of 10,000 lb/day of phthalic anhydride. It will be a multitube type reactor with heat transfer salt circulated through its jacket at a temperature equivalent to the feed temperature.

The catalyst consists of 0.32 cm diameter spheres that have a bulk density of 0.84 g cm^{-3} and pack into a fixed bed with a void fraction of 0.4. The mass velocity of the gas through each tube will be 0.075 g $\text{cm}^{-2}\ \text{s}^{-1}$, which corresponds to an overall heat transfer coefficient between the tube wall and the reacting fluid of about 10^{-3} cal $\text{cm}^{-2}\ \text{s}^{-1}\ \text{K}^{-1}$.

(a) Show the chemical structures of the reactants and products. Give the relevant material, energy, and momentum balances for a plug flow reactor. Define all terms and symbols carefully.

(b) Determine the temperature, pressure, and naphthalene concentration in the reactor as a function of catalyst bed depth using a feed temperature of 610 K and tubes of various inside diameters, so that a maximum temperature of 673 K is never exceeded. Present results for several different tube diameters. What is the largest diameter tube that can be used without

exceeding 673 K? How many tubes will be required, and how long must they be to attain the desired conversion and production rates? For this optimal tube diameter, vary the feed temperature (615, 620 K) and naphthalene mole fraction (0.9 percent and 1 percent) to examine the effects of these parameters on reactor behavior.

(c) Combustion can often occur as an undesirable side reaction. Consider the subsequent oxidation of phthalic anhydride (PA) that also occurs in the reactor according to:

$$C_8H_4O_3 + 7.5\,O_2 \Rightarrow 2\,H_2O + 8\,CO_2$$

with rate: $r = k_2 C_{PA}$ where $k_2 = 4.35 \times 10^4 \exp(-10{,}000/T)$ cm^3 s^{-1} gcat^{-1} and $\Delta H_r = -760$ kcal mol^{-1}. Redo part (b) and account for the subsequent oxidation of PA in the reactor. Include the selectivity to phthalic anhydride in your analysis.

5. When exothermic reactions are carried out in fixed-bed reactors, hot spots can develop. Investigate the stability of the fixed-bed reactor described below for: (a) cocurrent coolant flow and (b) countercurrent coolant flow when the inlet coolant temperature (T_C^0) is 350 K and higher. Calculate the sensitivity by plotting the maximum temperature in the reactor versus the inlet coolant temperature (the slope of this line is the sensitivity). Which mode of cooling minimizes the sensitivity? (This problem is adapted from material provided by Jean Cropley.)

Data:
Reaction system (solid-catalyzed):

$$\underset{\text{(DT)}}{\text{Dammitol}} + \frac{1}{2}O_2 \overset{r_1}{\Rightarrow} \underset{\text{(VA)}}{\text{Valualdehyde}} + H_2O,$$

$$\underset{\text{(VA)}}{\text{Valualdehyde}} + \frac{5}{2}O_2 \overset{r_2}{\Rightarrow} 2CO_2 + 2H_2O,$$

with $\Delta H_{r_1} = -74.32$ kBTU/lbmol, $\Delta H_{r_2} = -474.57$ kBTU/lbmol. The rate expressions for these reactions are:

$$RT = \left(\frac{1}{T} - \frac{1}{373}\right) \Big/ 1.987$$

$$P_{O_2} = X_{O_2} P_T$$

$$P_{DT} = X_{DT} P_T$$

$$P_{VA} = X_{VA} P_T$$

$$r_1 = \frac{k_1 \exp[-k_2 RT] P_{O_2}^{k_3} P_{DT}^{k_4}}{1 + k_5 P_{O_2}^{k_6} + k_7 P_{DT}^{k_8} + k_9 P_{VA}^{k_{10}}} \text{ lbmol/(lbcat-h)}$$

$$r_2 = \frac{k_{11} \exp[-k_{12} RT] P_{O_2}^{k_{13}} P_{VA}^{k_{14}}}{1 + k_5 P_{O_2}^{k_6} + k_7 P_{DT}^{k_8} + k_9 P_{VA}^{k_{10}}} \text{ lbmol/(lbcat-h)}$$

where P_T is the total pressure and:

$$k_1 = 1.771 \times 10^{-3} \qquad k_8 = 1.0$$
$$k_2 = 23295.0 \qquad k_9 = 1.25$$
$$k_3 = 0.5 \qquad k_{10} = 2.0$$
$$k_4 = 1.0 \qquad k_{11} = 2.795 \times 10^{-4}$$
$$k_5 = 0.8184 \qquad k_{12} = 33000.0$$
$$k_6 = 0.5 \qquad k_{13} = 0.5$$
$$k_7 = 0.2314 \qquad k_{14} = 2.0$$

The governing differential equations are (the reader should derive these equations):

mass balances:

$$\frac{dX_i}{dz} = \frac{(NT) R_i \rho_B A_C \cdot \overline{MW}}{W} + \frac{X_i}{\overline{MW}} \frac{d\overline{MW}}{dz}, \; i = 1(DT), 2(VA), 3(O_2), 4(CO_2), 5(H_2O)$$

energy balance on reacting fluid:

$$\frac{dT_R}{dz} = \frac{-(NT) A_C (r_1 \Delta H_{r_1} + r_2 \Delta H_{r_2}) \rho_B - \pi (NT) d_t U (T_R - T_C)}{W \cdot \overline{C}_p}$$

energy balance on coolant:

$$\frac{dT_C}{dz} = \frac{(\text{mode}) \pi (NT) d_t U (T_R - T_C)}{F_C C_{pC}}$$

mole change due to reactions—reactions in the presence of inert N_2:

$$\frac{d\overline{MW}}{dz} = \sum_{i=1}^{NC} M_i \frac{dX_i}{dz} - 28 \sum_{i=1}^{NC} \frac{dX_i}{dz}$$

momentum balance [alternative form from Equation (10.2.3) that accounts for the losses from both the wall and catalyst particles]:

$$\frac{dP_T}{dz} = \frac{-\alpha^2}{(32.2)(144)} \left[\frac{150 \bar{\mu} u}{d_p^2} \frac{(1 - \bar{\varepsilon}_B)^2}{\bar{\varepsilon}_B^3} + \frac{1.75 \overline{MW} u^2}{\alpha R_g T_R d_p} \frac{(1 - \bar{\varepsilon}_B)}{\bar{\varepsilon}_B^3} P_T \right]$$

where

$$u = \frac{(359)(14.7)W \cdot T}{(273)(3600)(NT) \cdot A_C \cdot \overline{\text{MW}} \cdot P_T}$$

(conversion of mass flow rate to superficial velocity)

$$\alpha = 1 + \frac{2d_p}{3(1 - \bar{\varepsilon}_B)d_t}$$

X_i = mole fraction of component i

u = superficial velocity (ft/s)

T_R = reacting fluid temperature (K)(T_R^0 = inlet value)

T_C = coolant temperature (K) (T_C^0 = inlet value)

$\overline{\text{MW}}$ = mean molecular weight of the reacting gas

P_T = total pressure (psia) (P_T^0 = inlet value)

W = total mass flow rate (lb/h)

NT = number of reactor tubes

A_C = cross-sectional area of a reactor tube

d_t = diameter of tube

d_p = catalyst pellet diameter

ρ_B = bed density (lbcat/ft^3)

z = axial coordinate (ft)

R_i = net reaction rate of component i (lbmol/lbcat/h), for example, $R_1 = -r_1$, $R_2 = r_1 - r_2$, $R_3 = -0.5r_1 - 2.5r_2$: assumes effectiveness factors are equal to one

$\bar{\varepsilon}_B$ = porosity of bed

U = overall heat transfer coefficient (BTU/h/ft^2/°C)

mode = (+1) for cocurrent coolant flow, (−1) for countercurrent coolant flow

$F_C C_{pC}$ = coolant rate (BTU/h/°C)

$\bar{\mu}$ = reacting fluid viscosity (lb/ft/h)

$\bar{C}_p$ = gas heat capacity (BTU/lb/°C)

R_g = universal gas constant (psia-ft^3/lbmol/K)

NC = number of components = 5

i	Component	M_i
1	Dammitol	46
2	Valuadehyde	44
3	O_2	32
4	CO_2	44
5	H_2O	18

reactor	2500 tubes	$\frac{1}{12}$ ft (ID) × 20 ft (length)
W	100,000	lb/h
X_1	0.1	
X_3	0.07	
X_5	0.02	
remainder is N_2 (O_2 comes from air)		
$F_C C_{pC}$	10^6	BTU/(h-°C)
P_T^0	114.7	psia
T_R^0	353	K
d_p	0.25	inches (spherical)
ρ_B	100	lb/ft^3
$\bar{\varepsilon}_B$	0.5	—
$\bar{\mu}$	0.048	lb/(ft-h)
$\bar{C}_p$	0.50	BTU/(lb-°C)
U	120.5	BTU/(h-ft^2-°C)

6. Refer to the reactor system described in Exercise 5. Using the mode of cooling that minimizes the sensitivity, what does the effect of changing $\bar{\varepsilon}_B$ from 0.5 to 0.4 (a realistic change) have on the reactor performance?
7. If the effectiveness factors are now not equal to one, write down the additional equations necessary to solve Exercise 5. Solve the reactor equations without the restriction of the effectiveness factors being unity.